The 2010 IEEE/RSJ International Conference on
Intelligent Robots and Systems
October 18-22, 2010, Taipei, Taiwan

High Speed Electro-Hydraulic Actuator for a SCARA Type Robotic Arm

Migara H. Liyanage, Nicholas Krouglicof and Raymond Gosine

Department of Mechanical Engineering
Faculty of Engineering & Applied Science
Memorial University, Newfoundland, Canada

Abstract— **This study details the development of a high performance servo-hydraulic actuator for a Selective Compliant Assembly Robotic Arm (SCARA). The arm is intended for high speed food processing applications; specifically on-line poultry deboning. The system is mathematically modeled and simulated. Based on the simulation results, the hydraulic actuators are sized for optimal performance. A prototype actuator is subsequently designed, manufactured and experimentally evaluated. The tests results demonstrate that the prototype actuator is capable of producing unprecedented torques and associated accelerations relative to its size and mass. Comparable performance is not feasible with contemporary electrical actuators of similar size.**

Keywords: hydraulic rotary actuators, hydraulic servo systems, high speed robotics, SCARA arm, poultry deboning.

I. INTRODUCTION

Selective Compliance Assembly Robot Arm (SCARA) type robotic manipulators have been used extensively for industrial automation. These robots are capable of performing a wide variety of precise pick and place operations in a variety of industrial applications. Electric actuators are commonly used for joint control in SCARA type manipulators; however, the use of such actuators limits the performance in terms of speed and payload. Some of the industries (eg. poultry processing) require higher production capacities which calls for greater manipulator speeds. This study proposes the development of a high speed SCARA type robot with servo-hydraulic actuators for joint control.

The robot in this study is for deboning of poultry parts in a production line. In a typical plant a conveyor belt transports up to 100 poultry parts per minute at a speed of 0.4 m/s. In modern processing facilities, x-ray technology is used to check for the position and orientation of deeply imbedded bone fragments. Currently, the physical deboning operation is manually performed. Proposed actuator will drive the two revolute joints of a Selective Compliant Assembly Robot Arm (SCARA) which will position the cutting blade assembly for the deboning operation. The motion generated by these actuators have to be fast, accurate, smooth, and non-oscillatory.

An actuator suitable for this SCARA arm should be of light weight, compact in size and capable of reaching higher speeds. The end effector of this arm should be easier to control for accurate positioning. It should also be suitably robust for the operation in demanding environments such as those found in the food processing industry.

Hydraulic actuators are capabile of producing a high power-to-weight ratios (approximately 5 times) and power-to volume ratios (approximately 10 to 20 times) larger than comparable electric motors. The torque to inertia ratio is also large with resulting high acceleration capability [1]. Hydraulics is preferred over electric actuators when higher speeds of operation is required with fast starts, stops and speed reversals [2], [1].

There is a clear lack of stuides on servo-hydraulics considering actual industry related problems. Nevertheless, most studies on servo-hydraulics have considered issues related to linear actuators [3], [4] and [5]. Out of these only a few studies have used servo-hydraulic actuators to drive manipulators. Bu and Yao [6], considered linear actuators for driving revolute joints. Linear actuators on revolute joints limit displacement. When speed is an important factor linear actuators may limit performance. There are limited number studies on rotary actuators Heintze [7], Bilodeau [8] and [9]. These studies have considered modeling and control of single vane rotary actuators. There has also been a study considering the development of a 6-DOF manipulator with hydraulic actuators using water [10]. However, it was developed for large pay load handling and does not consider high speed operation. None of these studies have either proposed a double vane rotary hydraulic actuator suitable for continuous high speed manipulator applications or detailed design of such a high performance actuator.

An important stage towards automation is establishing accurate dynamical models of the system [9]. Therefore, in this study a mathematical model for the system was formulated and modelled using MATLAB-SIMULINK® toolbox. Based on the results of the simulation, the size of the required actuator was estimated. The detailed design of the actuator components was carried out next. The actuator was manufactured and tests were carried out in order to validate the proposed model. A simple PID controller was used for initial tests.

This paper is organized as follows: A brief introduction is provided in section 1. Section 2 details the mathematical formulation of the proposed system model. In section 3, a brief overview of the simulation results is presented. The details of the actuator design and fabrication of the unit is presented next. In section 5 experimental results from actual testing of the actuator and a validation of the theoretical model is presented. Conclusions are presented in final section.

II. PROBLEM FORMULATION AND THE DYNAMIC MODEL

The actuator proposed is a double vane rotary hydraulic unit. The torque produced and the direction of rotation of the actuator is controlled by a high response electro-hydraulic servo valve. The links of the robotic arm are directly coupled to the actuator. The entire manipulator is composed of a hydraulic subsystem (servo valves and rotary actuators), SCARA arm and the controllers. Each of these have been modeled as separate components. This section presents an overview of the mathematical models for each subsystem.

This study considers only the 2 DOF movement of the links in x-y plane. The first actuator is stationary and directly drives link 1. The second actuator is fixed to link 1 and moves with the arm. Link 2 is considered to be fixed to the non-stationary actuator. Link 1 makes an angle θ_1 with x-axis while link 2 makes an angle of θ_2 with first link. The links of the robot are of length a_1 and a_2. The prismatic link is connected at the end of link 2 and moves in the $z-$ direction.

A. SCARA Robot Model

The Denavit and Hartenberg's convention is used to denote the joint angles and link parameters. The forward kinematics of the end effector is estimated using simple geometric relations. Hence:

$$p_x = a_1 cos\theta_1 + a_2 cos(\theta_1 + \theta_2) \tag{1}$$

$$p_y = a_1 sin\theta_1 + a_2 sin(\theta_1 + \theta_2) \tag{2}$$

The inverse kinematics of the robotic arm can also be obtained using basic geometric relations. Hence,

$$C = cos\theta_2 = \frac{p_x^2 + p_y^2 - a_1^2 - a_2^2}{2a_1 a_2} \tag{3}$$

$$D = \pm\sqrt{1 - cos^2\theta_2} \tag{4}$$

$$\theta_2 = atan2(D, C) \tag{5}$$

$$\theta_1 = atan2(p_y, p_x) - atan2(a_2 sin\theta_2, a_1 + a_2 cos\theta_2) \tag{6}$$

The generalized equation for toque of a serial manipulator is given by, [2],

$$\mathbf{T} = M(q)\ddot{\mathbf{q}} + \mathbf{V}(q, \dot{q}) + \mathbf{G}(q) \tag{7}$$

Where, $\mathbf{T}$ denotes the torque in each link. Joint variables, including the rotational angle (θ) of each joint is given by $\mathbf{q}$. $M(q)$ is the manipulator inertia matrix. $\mathbf{V}(q, \dot{q})$ is the velocity decoupling factor and $\mathbf{G}(q)$ is the vector of gravitational forces.

By considering the Lagrangian dynamics of a SCARA arm we can derive the following equations for the torques in link 1 (T_1) and link 2 (T_2) [2].

$$T_1 = [(\frac{m_1}{3} + m_2 + m_3)a_1^2 + (\frac{m_2}{3} + m_3)a_2^2 + (m_2 + 2m_3) a_1 a_2 cos\theta_2]\ddot{\theta_1} + [(\frac{m_2}{3} + m_3)a_2^2 + (\frac{m_2}{2} + m_3) a_1 a_2 cos\theta_2]\ddot{\theta_2} - (m_2 + 2m_3)a_1 a_2 sin\theta_2(\dot{\theta_1}\dot{\theta_2} + \frac{\dot{\theta_2}^2}{2}) \tag{8}$$

$$T_2 = [(\frac{m_2}{3} + m_3)a_2^2 + (\frac{m_2}{2} + m_3)a_1 a_2 cos\theta_2]\ddot{\theta_1} + (\frac{m_2}{3} + m_3)a_2^2\ddot{\theta_2} + \frac{1}{2}(m_2 + 2m_3)a_1 a_2 sin\theta_2 \dot{\theta_1}^2 \tag{9}$$

Where, the masses of the rotary links are denoted by m_1 and m_2, and the prismatic link is expected to be of mass m_3.

B. Hydraulic System Model

The hydraulic system consists of a double vane type rotary actuator, electro-hydraulic two-land-four-way servo valve, a hydraulic power unit and other basic components used for a hydraulic supply. The servo valve (MOOG® G761 series) acts as a regulating device for the oil flow. The hydraulic actuator consists of two compartments separated by a movable part or vane which produces rotary motion based on the direction of oil flow. A schematic diagram of cross section of the double vane actuator is shown in Fig. 1.

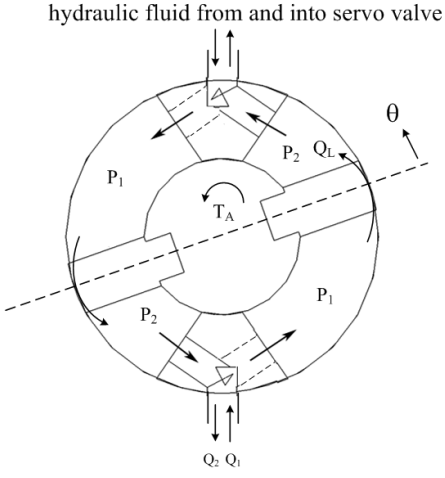

Fig. 1. A schematic diagram of cross section of the actuator

The basic mathematical relationships for hydraulic servo systems have been given in Merrit [1]. The dynamics of rotary hydraulic actuators coupled to a servo valve is

described by a number of theoretical relations as given in [7], [8] and [9].

When the vane has to be moved in a clockwise direction, the pressure in the left chamber has to be maintained higher than that of the right chamber. This is accomplished by displacing the spool valve so that it connects the oil supply and the first chamber of the actuator. This results in an oil flow from the supply into the left chamber and an out flow from the right chamber to tank. This flow is turbulent and the relation between the flow and effort variables (flow rate and pressure) is given by the square-root law [8]. Considering that the flow through the spool valve is similar to a flow through an orifice these relationships are given by [1],

$$Q_1 = c_d A_v \sqrt{\frac{2}{\rho}(P_s - P_1)}; Q_2 = c_d A_v \sqrt{\frac{2}{\rho}(P_2 - P_T)} \quad (10)$$

Where, Q_1 is the flow rate into the chambers, Q_2 is the flow rate from the chambers, c_d is the orifice flow coefficient, A_v is the area of valve opening, ρ is the density of fluid, P_s is the supply pressure, P_T is the tank pressure, P_1 is the pressure in chamber 1 and P_2 is the pressure in chamber 2.

In order to move the vane counter-clockwise, the spool valve moves in an opposite direction with flow into the right chamber. Thus,

$$Q_1 = c_d A_v \sqrt{\frac{2}{\rho}(P_1 - P_T)}, Q_2 = c_d A_v \sqrt{\frac{2}{\rho}(P_s - P_2)} \quad (11)$$

Cross-port leakage occurs when there is a high differential pressure across the two chambers of the actuator. This is given by,

$$Q_L = c_d A_L \sqrt{\frac{2}{\rho}(P_1 - P_2)} \quad (12)$$

Where, Q_L is the oil leakage rate and A_L is the area of oil leakage.

The area of the spool valve opening is a function of the spool displacement. Thus,

$$A_v = K_v x_v \quad (13)$$

Where, A_v is area of the valve opening, K_v is circumference of the cylindrical spool and x_v is spool displacement.

Furthermore, when the system is subjected to high supply pressures the total system including the actuator and conduits expand. Using the principles of continuity and fluid compressibility, pressure can be related to flow rate as follows [1],

$$P_1 = \frac{\beta}{V_1} \int Q_1 - D_M \dot{\theta} - Q_L \, dt; P_2 = \frac{\beta}{V_2} \int Q_L + D_M \dot{\theta} - Q_2 \, dt \quad (14)$$

Where, P_1 and P_2 denote pressure in chambers 1 and 2, V_1 and V_2 denote the initial volume in chambers 1 and 2, β denotes the effective bulk modulus of the system, D_M denotes the actuator displacement coefficient and $\dot{\theta}$ denotes angular velocity of the revolute joints.

The torque available to rotate the arm is the torque resulting from the pressure difference across the vane less the torque required to overcome viscous friction of the fluid and Coulomb friction and/or stiction torque of the actuator shaft. Therefore, by considering torque balance,

$$T_A = D_M(P_1 - P_2) - \sigma\dot{\theta} - c_t(\theta - \theta_f) + T_c \quad (15)$$

Where, T_A is the net actuator torque, σ is the viscous friction coefficient of oil, c_t is the torsional stiffness of the connecting shaft between the actuator and robotic link, θ_f is the final position of the actuator and T_c is the coulomb friction torque.

C. Controller design

For controlling the robot arm, PID based independent controllers are proposed for each joint. For a given joint angle using the PID independent joint control law,

$$u = \frac{K_p}{T_i} \int e \, dt + K_p T_d \frac{de}{dt} + K_p e \quad (16)$$

Where, u is the servo valve current, K_p, is the proportional gain, and T_d and T_i are the derivative and reset times, respectively.

A basic schematic diagram of the system framework is presented in Fig. 2. The system model was implemented using the MATLAB-SIMULINK® toolbox which has the capability of numerically solving nonlinear system models. A servo valve pressure of 20.7 MPa (3000 psi) is considered for simulation. It was assumed that the system operates with no friction and viscous forces. Using the system model, the control parameters were tuned to obtain a satisfactory dynamic response (less than 2 % error from desired joint angle). The system was tested for various step input values which produced end effector displacements throughout the operating envelope of the robot. Based on the simulation results, an optimal value for the displacement coefficient of the actuator was estimated.

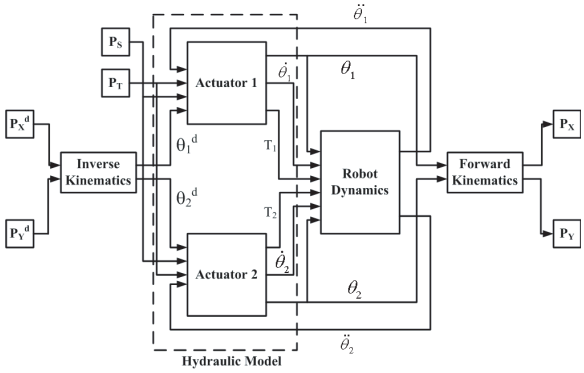

Fig. 2. Schematic drawing with components of the simulated system.

III. SIMULATION RESULTS

The overall system was capable of reaching controlled average velocities of up to 4.8 $\mathrm{m/s}$. Following the same trajectory the instantaneous velocity can reach peak values as high as 6.1 m/s. The above velocities are for an end effector displacement of 1.13 m. The tip velocity of the robot was found to be a much greater value when the robot moves over larger distances. The reason for this being that the actuator will reach high pressures for a longer time period only if it has to travel greater distances. The higher the pressure differential, the higher the acceleration, and the faster the actuator moves the arm. The average and maximum velocity of the arm for various displacements is shown in Fig. 3. Over the same range of values for final end effector displacement, joints 1 and 2 can reach speeds of up to 490 $^{\circ}/\mathrm{s}$ and 550 $^{\circ}/\mathrm{s}$, respectively.

The hydraulic actuators are capable of producing extremely high torques. The toque in actuator 1 is generally greater than that of actuator 2 as it has to drive both links as well as the end effector. Over the range of values for end effector displacement, in joints 1 and 2 the torque can reach up to a maximum of 1470 Nm and 480 Nm, respectively. This is a large torque compared to the torque available from an electrically driven actuator of comparable size. The variation of torque with time in the two actuators when the end effector moves from point (0.9 m,0 m) to point (0.5 m,0.6 m) in the work envelope in response to a step input is illustrated in Fig. 4. The torque T_1 reaches a maximum of 770 Nm at time 0.014 s and then starts to decrease. It reaches zero torque at t=0.079 s and reverses direction in order to decelerate the system. This reverse torque will reach a maximum of 860 Nm at 0.104 s. Following a similar pattern the torque T_2 will be a maximum of 283 Nm at 0.015 s and have a maximum reverse torque of 245 Nm at 0.105 s.

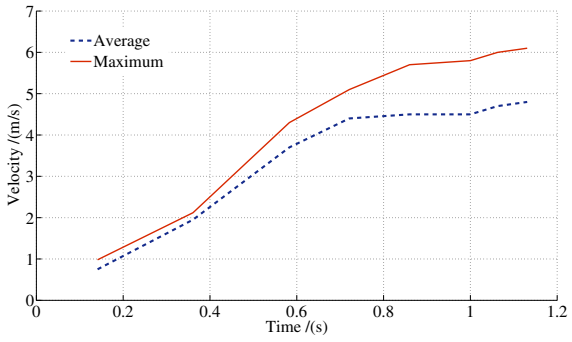

Fig. 3. Average and maximum velocity of the arm during displacement

IV. DESIGN AND FABRICATION OF THE ACTUATOR

The mechanical design software package SOLIDWORKS® was used in designing the various components of the actuator. Servo valves are connected to

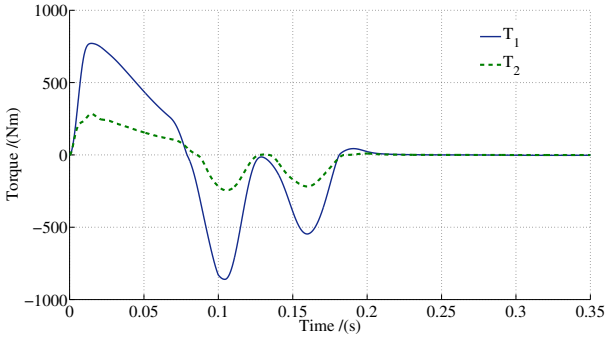

Fig. 4. Variation of actuator torque with time

a supply pressure of 20.7 MPa (3000 psi). The maximum pressure in the actuator greatly influences the mechanical design. Internal components of the actuator have to withstand such pressures. Stresses and strains on these components were tested at these pressures using the COSMOSWORKS® package.

The SCARA arm is designed with servo hydraulic actuators fixed to its revolute joints. The actuator displacement coefficient was obtained from the simulation as 4.0 x 10^{-5} $\mathrm{m^3/rad}$ (2.44 $\mathrm{in^3/rad}$). The size of the actuator is calculated based on this. This is the volume of hydraulic fluid displaced per unit rotation of the vane. It can also be viewed as the volumetric displacement required to generate the necessary torque at the specified system pressure. Estimation of this value is the first step of the actuator design process. The proposed actuator is a double vane rotary type actuator. A double vane rotary type actuator was considered for driving the shaft as it provides higher torque in a smaller mechanical package without excessive shaft forces. In order to minimize static friction, there are no seals between the vane and the housing. The leakage flow is minimized by closely controlling the manufacturing tolerances.

Using the estimated value for the actuator displacement coefficient, the inner diameter of the actuator housing was chosen to be 76.2 mm (3.0 inch) with an effective vane length of 4 inches. The thickness of the vanes was determined to be 12.7 mm (0.5 inch) based on stress considerations. The shaft dimensions were estimated based on the nominal dimensions of the vanes. The shaft was set at 38.1 mm (1.5 inches) in diameter internally (i.e., where it connected to the vanes) and 25.4 mm (1.0 inch) in diameter on the exterior. Instead of outside piping, a series of passageways were incorporated within the actuator housing to carry hydraulic fluid to and from the servo valve. To accommodate the passageways and other mechanical requirements, the outer dimensions of the housing was set at 114.3 x 114.3 x 101.6 mm (4.5 x 4.5 x 4.0 inches).

The cylindrical section of the actuator is divided into

two compartments by using two separators. The separators are triangular in shape and channel the hydraulic fluid in and out of the compartments. The hydraulic fluid applies pressure on the vanes, providing rotational movement to the shaft. A set of inner caps are used to close either sides of the actuator and to hold the separators in place. Two endcaps are used to seal either side of the housing. These end caps are secured to the housing using 8, 9.525 mm (3/8 inch) socket head cap screws. The end cap has a groove for incorporating a static O-ring as well as a rotary shaft seal in order to prevent leaks. The shaft is also mounted on two needle bearings to support the weight (i.e., forces in the z direction). The servo valve is installed on to a manifold which is fixed to the housing. The manifold has internal passageways to channel flow from the supply and tank. The actuator is fitted with external stops in order to prevent the vanes from striking the separators internally. The actuator shaft is connected to the robot links.

It is very important to design the system using light weight materials in order to minimize the inertia. Hence, an aircraft grade of aluminum (2024-T6 alloy) was considered for the housing, inner caps, end caps and the manifold. If a material like steel was used in place of this alloy the weight of the actuator would have increased by approximately 65 percent. Brass which has favorable impact and wear resistance properties was used for the chamber separators and vanes. High strength steel was used for the shaft.

All the components were checked for failure using the COSMOSWORKS® finite-element package. It was checked for expansion and deformation at the rated operating pressure. This actuator was fabricated at the Division of Technical Services at Memorial University.

The complete actuator including servo valve weighs approximately 6.9 kg. A brushless direct drive rotary KOLLMORGEN GOLDLINE DDR ®(DH143M) series electric motor that can produce almost same output (340 Nm of continuous torque) is 123 kg in weight and has a diameter of 360 mm (14.2 in) and a length of 340 mm (13.5 in). The rotor inertia of our actuator is 0.0025 kgm^2 while it is 0.542 kgm^2 for the given electric motor. The commercially available Micromatic® (SS-1 model) double vane rotary hydraulic actuator with same displacement coefficient, is around 9.75 kg in weight. It does not have external locks, integrated servovalve or the feedback device which would significantly increase the weight. The commercial actuator used a vane seal to control leaks between the chambers. However, it could introduce static friction to the system. The prototype actuator is custom built for a SCARA type robotic arm. An exploded view of the actuator is shown in Fig. 5.

V. RESULTS FROM TESTING OF THE ACTUATOR

For preliminary testing, an MTS® 407 controller by MTS® Systems Corporation was used. It is a specifically

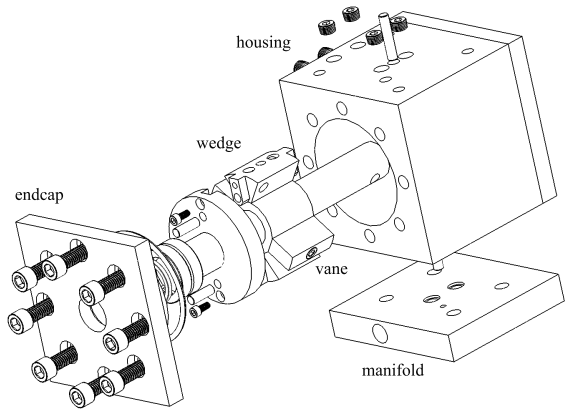

Fig. 5. An exploded view of the double vane rotary actuator

designed analog controller for hydraulic systems. Since this controller only accepts analog feedback devices, a servo potentiometer coupled to the end of the shaft was employed to provide feedback to the controller on the angular position of the arm. The servo valve is mounted directly on the manifold. Based on the error between actual and desired positions, a command signal is sent from the controller to the servo valve which translates into a spool displacement resulting in fluid flow into the actuator. The actuator compartments are fitted with pressure transducers. Experimental setup of the actuator and mass with hydraulic supply is shown in Fig. 6.

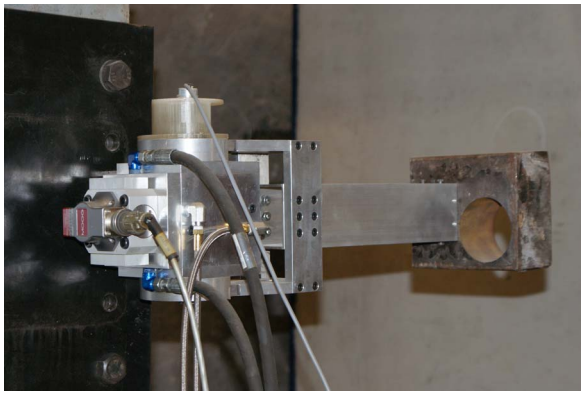

Fig. 6. The experimental setup

The system performance was evaluated for different wave forms, spans and a range of controller gains. As with many servo-hydraulic control systems, satisfactory control was achieved with proportional control alone. This section provides an analysis of the system response to different values of proportional gain. The controller records the feedback signal of the potentiometer and command signal to the servo valve over time. Based on these values, the desired and actual positions of the actuator was estimated. The pressure in the two chambers of the actuator over time was measured by means of the pressure transducers. Based

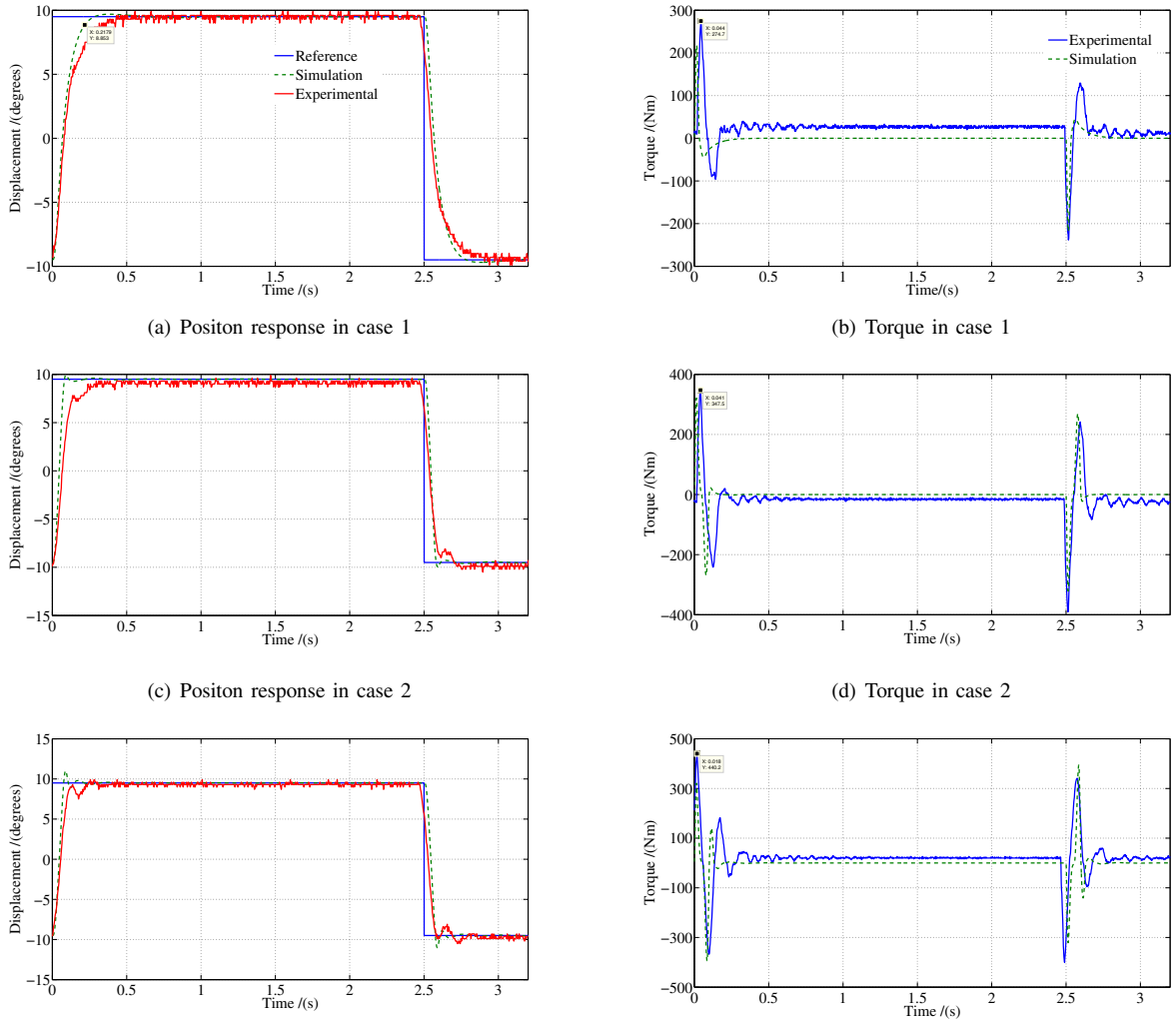

(a) Positon response in case 1

(b) Torque in case 1

(c) Positon response in case 2

(d) Torque in case 2

(e) Positon response in case 3

(f) Torque in case 3

Fig. 7. The system response and actuator torque to a given step response at different values for gain

on the pressure difference the actuator torque was calculated.

The system response was obtained for a square waveform which has a span of 18^o and a frequency of 0.2 Hz. Only the proportional gain was used while the integral and derivative gains were set to zero. The proportional gain was set to vary from low to high values. These will be denoted as cases 1,2 and 3 (C1,C2 and C3). The variation of angular displacement and torque over time for these controller gains are shown in Fig. 7. These figures provide a comparison of the reference angular displacement and torque between experimental and simulation values. The actual pressure of hydraulic supply in the lab was 14.9 MPa (2160 psi). Therefore, the simulation shown corresponds to this system pressure. A mass of 13 kg fixed to the end of the link was used to represent the mass of the manipulator.

The actuator response to this step input is shown in Fig.s 7(a), 7(c) and 7(e). According to the simulation the system reaches steady state (an angle of 17.64^o) in 0.217 s, 0.077 s and 0.074 s in cases 1, 2, and 3 respectively. Experimental results showed that it would take 0.320 s, 0.239 s and 0.117 s for cases 1,2 and 3, respectively in order to reach the same position. The torque produced by the actuator can be calculated using the pressure difference measured from the pressure transducers. The variation of actuator torque is shown in Fig. 7(b), 7(d) and 7(f). The negative values for torque in these figures indicate that it acts in a reverse direction. According to the simulation the actuator torque reaches a maximum of 220 Nm, 320 Nm and 395 Nm in cases 1,2 and 3, respectively. The experimental results indicate that the actuator is capable of producing torques of up to 270 Nm, 390 Nm and 440 Nm in the respective cases 1,2 and 3. The peak torque here is given considering the total time horizon and not the corresponding values for experimental and simulation cases. The negative torque basically acts as a braking torque to stop the output shaft. The experimental results have a close

resemblence with the mathematical simulation over the range of values considered for propotional gain. Therefore, the simulation results appear to validate the mathematical model.

There may be several reasons for the discrepancy between the actual and simulation values. The mathematical model developed was based on several assumptions. The tank pressure was assumed to be negligible in the model; however, this may not be the case in an actual hydraulic power unit particularly if it is not in close proximity to the actuator. The effects of friction were also neglected in the simulation. These assumptions are not strictly valid in the actual system. The noise produced by the potentiometer is also relatively high as seen in the experimental response curves. This noise can result in a pressure fluctuations with associated variations in torque. Other potential sources of error include vibration of the vertical structure on which the arm was mounted for testing.

VI. CONCLUSIONS AND FUTURE WORK

The main objective of this paper is to propose a high speed hydraulic actuator for robotic applications. This actuator will be used in a SCARA type robotic arm for poultry deboning applications. The actuator size was estimated based on a simulation of the complete robot manipulator. The actuator was designed and manufactured using light weight materials and experimentally tested to verify performance. The tests showed that a proportional controller alone provides satisfactory control of the single actuator system. The test results demonstrate that the prototype actuator is capable of producing torques of up to 440 Nm at the system pressure of 14.9 MPa (2160 psi) and with a load of 13 kg. The test results also validated the proposed mathematical model for the actuator.

Electric counterparts do not have high power to weight ratios. For example KOLLMORGEN®-DH143M electric motor has a power to weight ratio of 2.8 Nm/kg while the same for prototype actuator is 63.8 Nm/kg. The prototype actuator is also compact (114.3 x 114.3 x 127.0 mm) in size and light weight (6.9 kg) compared to other commercial actuators of similar configuration. This is also custom built to suit its application in a SCARA type robotic arm.

This study considered a simple PID controller for joint control. A trial and error method was used to tune the parameters of the controller; however, a more robust and accurate method is needed to properly tune these parameters. In addition, a linear controller such as the one employed here does not provide the best performance for a non-linear system with varying inertia. Therefore, a more suitable control strategy will be proposed in future studies.

VII. ACKNOWLEDGEMENT

This work is supported by the Natural Sciences and Engineering Research Council of Canada (NSERC) and Baader-Canpolar Inc., St Johns, NL, Canada. We would also like to thank Ken Brown, Mathew Curtis, Tom Pike and Don Taylor for their support. Authors would like to thank the anonymous reviewers for their comments. However, only the authors are responsible for any remaining errors or omissions.

REFERENCES

[1] H. Merrit, *Hydraulic control systems*. John Wiley & Sons, Inc., 1967.
[2] L. Tsai, *Robot Analysis: The Mechanics of Serial and Parallel Manipulators*. New York: John Wiley & Sons, 1999.
[3] P. Nakkarat and S. Kuntanapreeda, "Observer-based backstepping force control of an electrohydraulic actuator," *Control Engineering Practice*, vol. 17, no. 8, pp. 895 – 902, 2009.
[4] G. P. Liu and S. Daley, "Optimal-tuning pid control for industrial systems," *Control Engineering Practice*, vol. 9, no. 11, pp. 1185 – 1194, 2001.
[5] C. Kaddissi, J.-P. Kenne, and M. Saad, "Identification and real-time control of an electrohydraulic servo system based on nonlinear backstepping," *Mechatronics, IEEE/ASME Transactions on*, vol. 12, no. 1, pp. 12–22, Feb. 2007.
[6] F. Bu and B. Yao, "Nonlinear adaptive robust control of hydraulic actuators regulated by proportional directional control valves with deadband and nonlinear flow gains." Proceedings of the American Control Conference, 2000, pp. 4129–4133.
[7] J. Heintze, G. Van Schothorst, A. Van der Weiden, and P. Teerhuis, "Modeling and control of an industrial hydraulic rotary vane actuator," IEEE. Proceedings of the 32nd Conference on Decision and Control, 15-17 December 1993, pp. 1913–1918.
[8] G. Bilodeau and E. Papadopoulos, "Development of a hydraulic manipulator servoactuator model: simulation and experimental validation," *Robotics and Automation, 1997. Proceedings., 1997 IEEE International Conference on*, vol. 2, pp. 1547–1552 vol.2, 20-25 Apr 1997.
[9] P. La Hera, U. Mettin, S. Westerberg, and A. Shiriaev, "Modeling and control of hydraulic rotary actuators used in forestry cranes," in *Robotics and Automation, 2009. ICRA '09. IEEE International Conference on*, May 2009, pp. 1315–1320.
[10] Y. Measson, O. David, F. Louveau, and J. P. Friconneau, "Technology and control for hydraulic manipulators," *Fusion Engineering and Design*, vol. 69, no. 1-4, pp. 129 – 134, 2003, 22nd Symposium on Fusion Technology. [Online]. Available: http://www.sciencedirect.com/science/article/B6V3C-48V94C4-Y/2/b369b903b9db5eb4c7c1f54095d72f7e